Friction Compensation and $\mathcal{H}_\infty$–Based Torque Control of Harmonic Drive Systems

H.D. Taghirad† and P.R. Bélanger‡
Center for Intelligent Machines,
Department of Electrical Engineering,
McGill University, Montréal, H3A 2A7
† taghirad@cim.mcgill.ca, ‡ pbelange@fgsr.lan.mcgill.ca

Abstract—

A harmonic drive is a compact, light–weight and high–ratio torque transmission device which is used in many electrically actuated robot manipulators. In many robotic control strategies it is assumed that the actuator is an ideal torque source. However, converting harmonic drive systems to ideal torque sources is still a challenging control problem for researchers. In this paper the torque control of harmonic drive system is examined in detail. An empirical nominal model for the system is obtained through experimental frequency response estimates, and the deviation of the system from the model is encapsulated by multiplicative uncertainty. A robust torque controller is subsequently designed in an $\mathcal{H}_\infty$ –framework and implemented employing Kalman filtered torque estimates. Exceptional performance results are obtained from the time and frequency response of the closed–loop system. To further improve the performance of the system, a model–based friction–compensation algorithm is implemented in addition to the robust torque control. It is shown that the friction–compensation shrinks the model uncertainty at low frequencies. Hence, the performance of the closed–loop system is improved for tracking signals with low–frequency content.

I. Introduction

Robot manipulators require actuators with high torque capability at low velocities. On the contrary, DC–motors provide their operating torque only at high velocities. Many electrically actuated robots therefore, use a gear transmission to increase the torque and decrease the operating speed. Among gear transmissions, harmonic drives are high–ratio, compact and light–weight mechanisms with almost no backlash. These unique performance features of harmonic drives has captured the attention of designers. This mechanical transmission, occasionally called "strain-wave gearing", employs a continuous deflection wave along non-rigid gear, named *flexspline*. This allow for gradual engagement of gear teeth, but reduce the transmission stiffness and introduce vibration at the output shaft. This vibration appears in output speed and torque of the system, and is significant at the resonant frequency of the system [5].

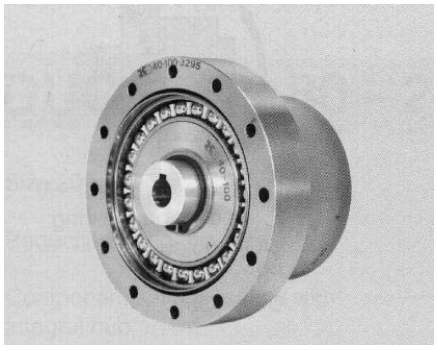

Fig. 1. Harmonic drive

In numerous robotic control techniques such as feedback linearization, computed torque method and some adaptive control schemes, actuator torque is taken to be the control input [10], [12], [11]. The physical variable being manipulated in practice, however, is not torque but armature current in a DC motor, for instance. For harmonic drive systems the relation between output torque and input current possesses nonlinear dynamics, due to the flexibility, Coulomb friction and structural damping of the harmonic drive [14]. Therefore, it is desired to improve this input/output relation by torque feedback, and to convert the system to an ideal torque source with a flat frequency response over a wide bandwidth. Brigdes et al. [2], Kaneko et al. [6], Kazerooni [8] and Kubo et al. [9] are representative of researchers who worked on this problem. Bridges used a very simple linear model for the system, with PD torque control [2]. His results show some improvement in tracking error, but insufficient performance near resonant frequency. Kaneko also based his analysis on a simple model of the system, but included nonlinear stiffness in the system [6]. He then applied a feedforward loop to adjust for nonlinear stiffness and then a pure gain torque feedback to shape the performance. Kazerooni considers a simple linear system for the harmonic drive, and used a sensitivity loopshaping technique to design a linear controller for the system [8]. Kubo et al. examined friction–compensation on harmonic drives, and presented a stability analysis with experimental verification of the improved performance of the system [9].

In this paper torque–control of harmonic drive system under free motion is restudied in details. First for the system. It is shown that an empirical linear model obtained from experimental frequency responses of the system, and an uncertainty characterisation of this model is sufficient to build a robust torque controller. Mixed–sensitivity problem is solved for the controller design, and the proposed controller is implemented and experimented. The closed–loop performance in time and frequency domains is shown to be exceptionally good. Then, in order to further improve the performance of the system, a model–

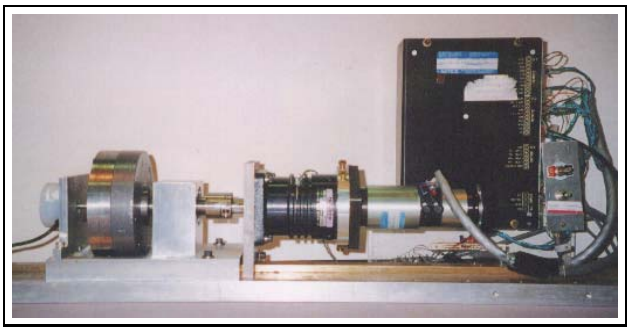

Fig. 2. Picture of the experimental setup and its schematics

based friction–compensation algorithm is implemented in addition to the robust torque control. It is shown that the friction–compensation shrinks the model uncertainty at low frequencies. Hence, the performance of the closed–loop system is improved for tracking signals with low–frequency content.

II. Experimental Setup

A harmonic drive testing station is employed to monitor the behaviour of the system in free–motion experiments. A picture of the setup and its schematics are illustrated in Figure 2, in which the harmonic drive is driven by a DC motor, and a load inertia is used to simulate the robot arm for unrestrained motion. In this setup, a brushed DC motor from Electro–Craft is used. Its weight is 1360 grammes, with maximum rated torque of 0.15 Nm, and torque constant of 0.0543 Nm/amp. The servo amplifier is a 100 Watts Electro–Craft power amplifier. The harmonic drive is from RHS series of HD systems, with gear ratio of 100:1, and rated torque of 40 Nm.

The setup is equipped with a tachometer to measure the motor velocity, and an encoder on the load side to measure the output position. The current applied to the DC motor is measured from the servo amplifier output and the output torque is measured by a Wheatstone bridge of strain gauges mounted directly on the flexspline [4]. The details of torque sensing technique is elaborated in [17]. These signals were processed by several data acquisition boards and monitored by a C-30 Challenger processor executing compiled computer C codes. Moreover, Siglab [3], a DSP hardware linked to Matlab, is used for frequency response analysis of the system. This hardware is capable of generating sine-sweep, random, and chirp function inputs to the system, and analyse the output signals and generate online frequency response estimates of the system.

III. $\mathcal{H}_\infty$–Based Torque Control

To capture the system dynamics accurately, it is necessary to consider nonlinear models for friction and structural damping [14]. However, for the purpose of control, a simple linear model for the system is sufficient for synthesis. An empirical nominal model for the system is derived using experimental frequency response on the system, as addressed in detail in [15], [16]. Moreover, the frequency response variation of the system is encapsulated by multiplicative uncertainty. Figure 4 illustrates some experimental frequency responses of the system with different input amplitudes, the nominal model frequency response, and the variations in frequency response using multiplicative uncertainty.

The nominal model for the system is found to be a third order stable and minimum phase transfer function as follows:

$$\frac{\text{Torque}}{\text{Ref Voltage}} = \frac{243.16\ (s+2.415)}{s^3+171.19s^2+1.24\times10^4 s+1.47\times10^5} \tag{1}$$

which has three stable poles at -14.465, and $-78.363 \pm 63.288j$. The uncertainty weighting function which is the upper bound of different uncertainty frequency plots is approximated by a second order system as:

$$\mathbf{W}(s) = \left(\frac{s+120}{145}\right)^2 \tag{2}$$

The control objective can be defined as *robustly stabilizing the system, while maintaining good disturbance attenuation and small tracking error, despite the actuator saturation.* This objective is well–suited to the general $\mathcal{H}_\infty$ problem. This control objective is translated into the general $\mathcal{H}_\infty$ problem and solved using μ–synthesis toolbox of Matlab in a similar way as elaborated in [16]. As illustrated in Figure 3 performance–weighting functions are selected considering the physical limitations of the system. The actuator saturation–weighting function is considered to be a constant, by which the maximum expected input amplitude never saturates the actuator. Its value is estimated to be 0.002 for free load experiments. The sensitivity–performance function is assigned to be $\mathbf{W}_s(s) = \frac{s+280}{5(s+2.8)}$. This weighing function indicates that at low frequencies, the closed–loop system should reject disturbance at the output by a factor of 20 to 1. Expressed differently, steady-state tracking errors due to step input should be less than 5 % or less.

The controller designed using μ–synthesis toolbox of Matlab has the following transfer function:

$$\mathbf{C}(s) = \frac{8.345\times10^5(s+14.5)(s+78.4\pm63.3j)}{(s+1.83)(s+2.8)(s+273.23)(s+1.0\times10^4)} \tag{3}$$

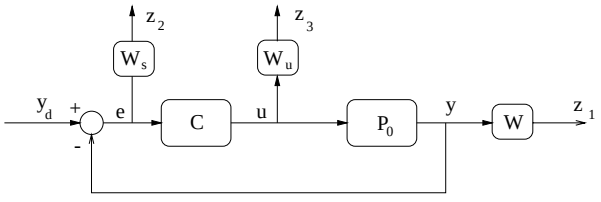

Fig. 3. Block diagram of system in $\mathcal{H}_\infty$ framework

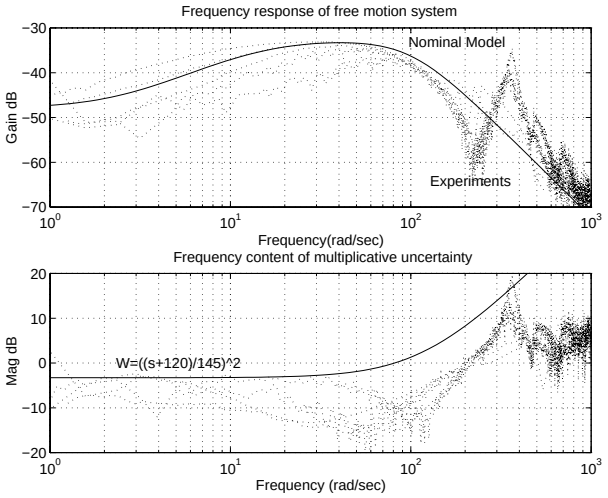

Fig. 4. Frequency response of the system, nominal model, and multiplicative uncertainty

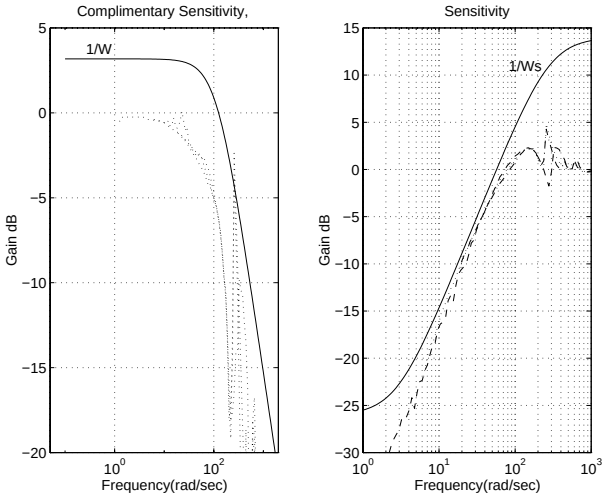

Fig. 5. Closed–loop frequency performance

The controller zeros cancel the stable poles of the nominal plant, while the poles shape the closed–loop sensitivity function to lie beneath the weighting function $\mathbf{W}_s$.

IV. Controller Performance

To verify the controller performance both simulations and experiments have been utilized. Here we only report the experimental results which are more convincing. To implement the controller in practice, bilinear discretization is performed with one kHz sampling frequency. The performance of the closed–loop system is evaluated in both frequency and time domain. The frequency domain performance of the closed–loop system is obtained from the closed–loop frequency response of the system and is illustrated in Figure 5. The experimental sensitivity and complementary sensitivity functions are shown to be underneath the inverse of sensitivity weighting function $\mathbf{W}_s$, and uncertainty weighting function $\mathbf{W}$ respectively. Also the Nyquist plot for the loop-gain of the system is derived from the experimental sensitivity functions, and the phase margin for the system is found to be about 80^o. These results are an experimental verification of the $\mathcal{H}_\infty$ design claim to preserve robust stability while shaping the performance as desired.

The time responses of the system to different reference input signals are illustrated in Figure 6. The dotted lines are the measured output torque of the system, which is tracking the solid line, the reference command, very fast and accurately. Although our designed bandwidth was about 3 rad/sec, sinusoid inputs up to 10 Hz (62 rad/sec) are shown to be well tracked. The step response is fast with a steady–state error less than 5 %, as required. Tracking of the system to triangular signal is especially sharp at the edges, and the tracking to an arbitrary signal is shown to be very fast and well-behaved. The main difference between harmonic drive free motion experiments and the constrained motion experiments is that in free motion case the output torque is relatively small, and therefore, the signal to noise ratio are higher than that for constrained motion case, as given in [16]. However, for both cases fast and accurate closed loop responses are obtained using $\mathcal{H}_\infty$ controllers.

V. Friction–Compensation

To improve the closed–loop performance of the system under free–motion, we applied a friction–compensation algorithm to the open-loop system. As illustrated in Figure 4, the frequency response of the system under free–motion possess significant variations at low frequencies. This is mainly caused by the nonlinear behaviour of friction which is dominant at low frequencies. In [14], a complete model of harmonic drive friction was presented as Coulomb, viscous and Stribeck friction. Friction parameters were carefully identified from experiments, and it is illustrated that the effect of Coulomb and Viscous friction is significant for free–motion experiments, while Stribeck friction remains apparent in low–velocity experiments. Therefore, in the sequel study we only compensate for Coulomb and viscous friction.

A. Friction–Compensation Algorithm

The equation governing the harmonic drive friction can be written as [14]:

$$T_{fric}(\dot\theta) = T_{v_n} u_{-1}(-\dot\theta)\dot\theta + T_{v_p} u_{-1}(\dot\theta)\dot\theta + T_{s_n} u_{-1}(-\dot\theta)\text{sign}(\dot\theta) + T_{s_p} u_{-1}(\dot\theta)\text{sign}(\dot\theta) \quad (4)$$

where

$$u_{-1}(x) = \begin{cases} 1 & \text{if } x > 0 \\ 0 & \text{if } x \le 0 \end{cases} \quad (5)$$

T_{v_n} and T_{v_p} are the viscous friction coefficient depending on the direction of the velocity, and T_{s_n} and T_{s_p} are the

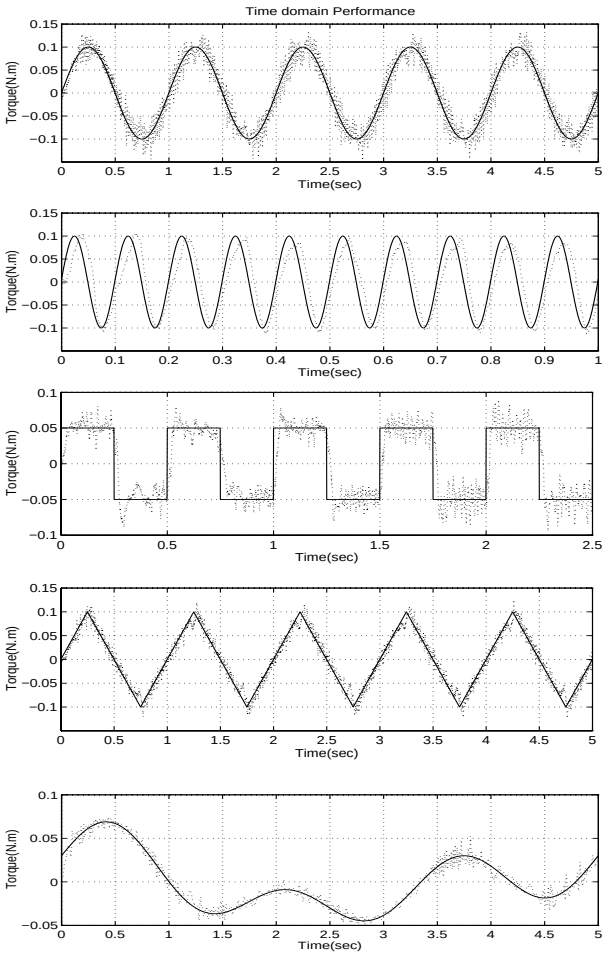

Fig. 6. Closed–loop time performance of the system employing Kalman filtered torque and robust controller

Coulomb friction coefficients as illustrated in Figure 7. For the McGill setup the identified parameters are [13]: $T_{v_n} = 3.5 \times 10^{-4}$, $T_{v_p} = 3.7 \times 10^{-4} (N.m.sec/rad)$, $T_{s_n} = 4.4 \times 10^{-2}$, and $T_{s_p} = 4.6 \times 10^{-2} (N.m)$.

The idea of friction–compensation is to estimate the friction torque at each instant from the measured velocity of the system, and to increase the reference command to the servo-amp corresponding to the estimated friction. Ideally, estimated friction should be equal to the actual friction; however, the magnitude of the friction depends on the operating condition, and special care must be taken so that over–compensation does not occur, which introduces instability into the system. For our experimental setup only 90 % of the estimated friction is compensated in order to avoid over–compensation, as suggested by Kubo et al. [9]. Another practical issue in the friction–compensation algorithm is the method of implementing hard nonlinear Coulomb friction. The estimated friction will change sign as velocity crosses zero. In practice, however, the velocity measurement is sampled, and hence, zero velocity crossing may never coincide at the sampling instants. Moreover, the velocity signal is always contaminated with noise, and at low velocity several unrealistic zero crossing may appear.

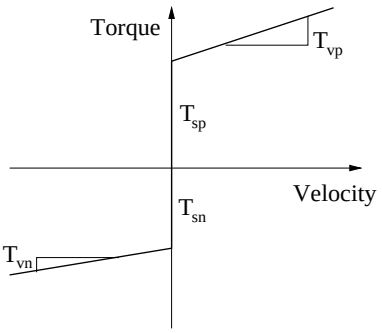

Fig. 7. Identified Coulomb and viscous friction curve for harmonic drive systems

To avoid chattering in friction–compensation, a *threshold velocity* was introduced in the literature [1], [7] to smooth the hard nonlinearity of Coulomb friction. Including the threshold velocity $\dot{\theta}_t$ the final friction estimation function will be as follows:

$$T_{fric} = \begin{cases} T_{v_p}\dot{\theta} + T_{s_p} & \dot{\theta} > \dot{\theta}_t \\ T_{v_p}\dot{\theta} + T_{s_p} & |\dot{\theta}| \leq \dot{\theta}_t \quad \& \quad V_{ref} > 0 \\ T_{v_n}\dot{\theta} - T_{s_n} & |\dot{\theta}| \leq \dot{\theta}_t \quad \& \quad V_{ref} < 0 \\ T_{v_n}\dot{\theta} - T_{s_n} & \dot{\theta} > \dot{\theta}_t \end{cases} \tag{6}$$

in which V_{ref} is the reference voltage commanded to the servo–amp, and the threshold velocity is set to $\dot{\theta}_t = 1\ (rad/sec)$ for the experiments. Within the threshold velocity region the direction of the friction torque is determined by the sign of the reference command signal instead of the velocity. It is verified by experiments that this representation of the friction torque at low velocities eliminates the chattering problem.

Figure 8 illustrates the Block diagram of friction–compensation algorithm implemented on the setup. The corresponding reference command compensating for the friction is estimated by dividing the friction torque estimate by the motor torque constant $K_m(N.m/amp)$ and by the servo–amp gain $G_{amp}(amp/volt)$, as illustrated in Figure 8.

B. System Model and its Reduced Uncertainty

Similar to the free–motion case, an empirical nominal model for the system including the friction–compensation can be derived using experimental frequency response. Figure 9 illustrates the empirical frequency responses of the system with friction–compensation, including nominal model and its uncertainty weighting function. The effect

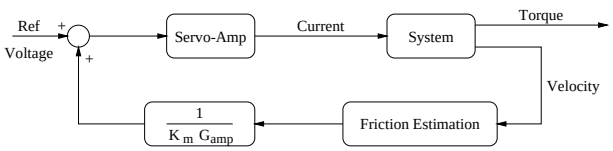

Fig. 8. Block diagram of the friction–compensation algorithm

of friction–compensation on the variation of the frequency response estimates at low frequencies is clearly seen when compared to Figure 4. The friction–compensated system behaves more linearly at low frequencies, and hence, the uncertainty of the system shrinks at low frequencies, from -3.3 dB to -10 dB. The uncertainty measure of the system is therefore, not only used in $\mathcal{H}_\infty$ synthesis to design the controller, but also as a gauge of the effectiveness of the friction–compensation algorithm.

A nominal model for the friction–compensated system is taken to be the following third–order stable and minimum–phase transfer function

$$\frac{\text{Torque}}{\text{Ref Voltage}} = \frac{109.4\ (s+1.363)}{s^3+96.06s^2+5159s+2.71\times10^4} \qquad (7)$$

which has three stable poles at -5.868, and $-45.096 \pm 50.953j$, and a DC–gain of -45.2 dB. The uncertainty weighting function is approximated by $\mathbf{W}(s) = \left(\frac{s+120}{213.4}\right)^2$.

C. $\mathcal{H}_\infty$–Based Torque Control

Similar to the free–motion case, for the friction–compensated system a controller is designed using an $\mathcal{H}_\infty$–framework. The sensitivity weighting function is assigned $\mathbf{W}_s(s) = \frac{s+530}{5(s+5.3)}$ with a bandwidth of 5.3 (rad/sec), which compared to 2.8 (rad/sec) bandwidth in free–motion system is a significant improvement. The 5 % steady state tracking error is maintained, while in another trial, it has been shown that 2 % tracking error assignment is also achievable, but with a bandwith of 1.75 (rad/sec). The actuator saturation–weighting function is set to be 0.002, the same as was assigned in system without friction–compensation. The controllers were designed using the μ–synthesis toolbox of Matlab by solving the mixed–sensitivity problem explained in § V-C. For friction–compensated system controller transfer function is:

$$\mathbf{C}_{FC}(s) = \frac{3.30\times10^6(s+5.8679)(s+45.10\pm50.95j)}{(s+1.27)(s+5)(s+318.86)(s+1.06\times10^4)} \qquad (8)$$

with a DC–gain of 72 dB.

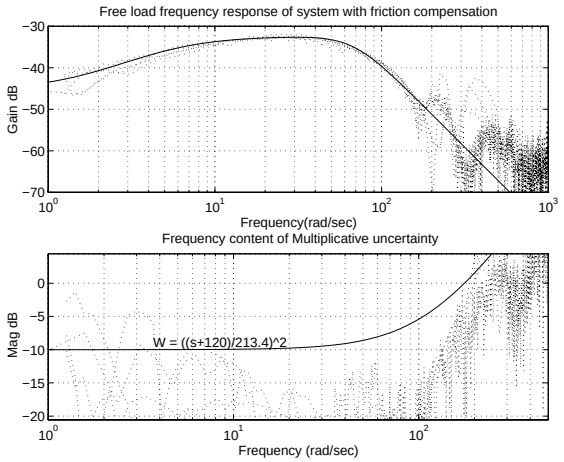

Fig. 9. Frequency response of the free–motion system with friction compensation, its nominal model, and multiplicative uncertainty

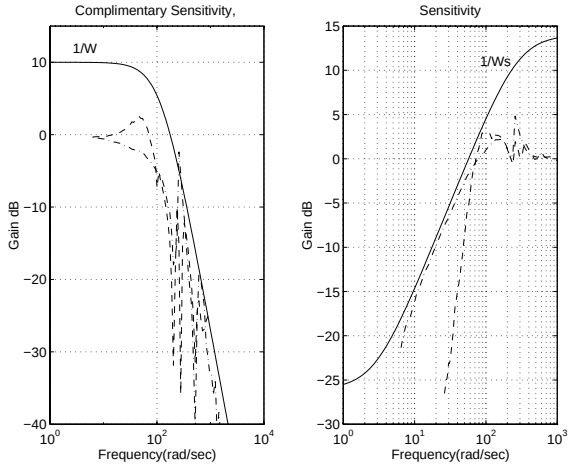

Fig. 10. Closed–loop frequency performance comparison of the system with and without friction–compensation; Dashed : With friction–compensation, Dash-Dotted : Without friction–compensation

VI. Closed–Loop Performance Comparison

To compare the performance of the closed–loop system with and without friction–compensation, frequency domain sensitivity and complementary sensitivity functions are shown in Figure 10. The friction–compensated system has a smaller sensitivity function at low frequencies, compared to the system without friction–compensation; however, its complementary sensitivity function shows larger overshoot close to the resonance frequency. Nevertheless, this is well below the inverse of the uncertainty weighting function, and hence, the robust stability has not deteriorated. The performance comparison of the system in time–domain is illustrated in Figure 11. For low–frequency sinusoid and triangular signals friction–compensation has improved the performance while for signals with high frequency content the performance is not improved, as illustrated for 10 Hz sinusoid and squared signals. Over all, for the applications where signals with low frequency content should be tracked, this comparison suggest that the friction–compensation will result in a superior performance. However, for the applications where high frequencies are involved (step response for instance) friction–compensation doesn't contribute to performance. This is because as illustrated in Figure 9 friction–compensation will linearize the system only at low–frequencies, and moreover, a percentage of the servo–amp power is consumed for the friction–compensation, so less power is available for high frequency trackings. In our experimental setup, depending on the output velocity, $12-25\%$ of the servo-amp power was utilized for friction–compensation algorithm.

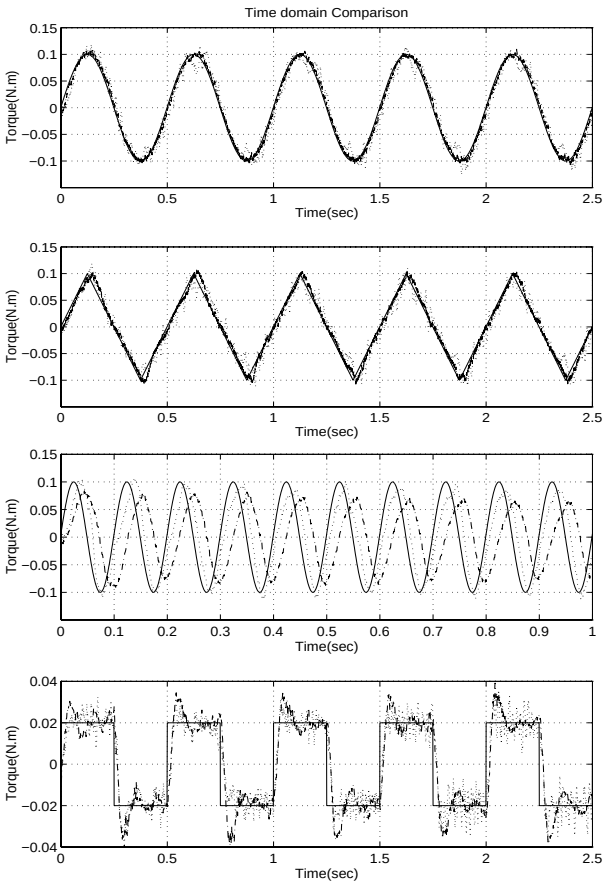

Fig. 11. Closed–loop time response comparison of the system with and without friction–compensation; Solid : Reference command, Dash-Dotted : With friction–compensation, Dotted : Without friction–compensation

VII. Conclusions

In this paper the torque control of harmonic drive systems for free motion case is examined in detail. To design a torque controller an empirical nominal model for the system is obtained through experimental frequency response estimates using kalman filtered torques as the output of the system. It is shown that by this means there is no need to resort to a nonlinear model for the system [14]. By this method not only a nominal model for the system can be proposed, but also the deviation of the nonlinear system from the nominal model can be encapsulated in a model uncertainty. This representation provides sufficient information to build a robust torque controller for the harmonic drive system. Solving the mixed–sensitivity problem for a tracking and disturbance attenuation objective, a fourth–order $\mathcal{H}_\infty$ controller is designed respecting the actuator saturation limits. By implementing the controller, the performance of the closed–loop system is evaluated experimentally. It is shown that the closed–loop system retains robust stability, while improving the tracking performance exceptionally well. To further improve the performance of the system for the free–motion case, a model–based friction–compensation algorithm is implemented. It is shown that compensation of estimated Coulomb and viscous friction reduces the system frequency response variations, and hence, model uncertainty. The uncertainty measure is therefore, not only used for control synthesis, but also as a quantitative indicator of the effectiveness of the friction–compensation algorithm. By comparison of the frequency and time domain performance of the system with and without friction–compensation, it is concluded that friction–compensation improves the performance of the system improved for tracking signals with low–frequency content.

References

[1] B. Armstrong-Helouvry, P. Dupont, and C. Canudas de wit. A survey of models, analysis tools and compensation methods for control of machines with friction. *Automatica*, 30(7):1083–1138, 1994.

[2] M.M. Bridges, D.M. Dawson, and S.C. Martindale. Experimental study of flexible joint robots with harmonic drive gearing. *Proceedings of the IEEE Conference on Control Applications*, 2:499–504, 1993.

[3] Signal Analysis Group. *DSP Technology Inc. Siglab Version 1.0.* DSP Technology Inc., 48500 Kato Road, Fremont, CA 94538-7385, 1994.

[4] M. Hashimoto, Y. Kiyosawa, H. Hirabayashi, and R.P. Paul. A joint torque sensing technique for robots with harmonic drives. *Proceeding of IEEE International Conference on Robotics and Automation*, 2:1034–1039, April 1991.

[5] T. Hidaka, T. Ishida, Y. Zhang, M. Sasahara, and Y. Tonika. Vibration of a strain-wave gearing in an industrial robot. *Proceedings of the 1990 International Power Transmission and Gearing Conference - New Technology Power Transmission, ASME Publications*, 1:789–794, 1990.

[6] K. Kaneko, T. Murakami, K. Ohnishi, and K. Komoriya. Torque control with nonlinear compensation for harmonic drive DC motors. *IECON Proceedings*, 2:1022–1027, 1994.

[7] D. Karnopp. Computer simulation of stick-slip friction in mechanical dynamic systems. *Journal of Dynamic Systems, Measurement and Control*, 107(1):100–103, 1985.

[8] H. Kazerooni. Dynamics and control of instrumented harmonic drives. *Journal of Dynamic Systems Measurement and Control - Transactions of the ASME*, 117(1):15–19, March 1995.

[9] T. Kubo, G. Anwar, and M. Tomizuka. Application of nonlinear friction compensation to robot arm control. *Proceeding of IEEE International Conference on Robotics and Automation*, 1:722–727, 1986.

[10] S. Nicosia and P. Tomei. On the feedback linearization of robots with elastic joints. *Proceeding of IEEE Conference on Decision and Control*, 1:180–185, 1988.

[11] M.W. Spong. Adaptive control of flexible joint manipulators. *Systems & Control Letters*, 13(1):15–21, Jul 1989.

[12] M.W. Spong, J.Y. Hung, S. Bortoff, and F. Ghorbel. Comparison of feedback linearization and singular perturbation techniques for the control of flexible joint robots. *Proceedings of the American Control Conference*, 1:25–30, 1989.

[13] Hamid D. Taghirad. *Robust torque control of harmonic drive systems.* PhD thesis, McGill University, March 1997.

[14] H.D. Taghirad and P.R. Belanger. An experimental study on modelling and identification of harmonic drive systems. *Proceeding of IEEE Conference on Decision and Control*, 4:4725–30, Dec 1996.

[15] H.D. Taghirad and P.R. Belanger. Intelligent torque sensing and robust torque control of harmonic drive under free–motion. *Proceeding of IEEE International Conference on Robotics and Automation*, 2:1749–54, April 1997.

[16] H.D. Taghirad and P.R. Belanger. Robust torque control of harmonic drive under constrained motion. *Proceeding of IEEE International Conference on Robotics and Automation*, 1:248–253, April 1997.

[17] H.D. Taghirad, A. Helmy, and P.R. Belanger. Intelligent built-in torque sensor for harmonic drive system. *Proceedings of the 1997 IEEE Instrumentation and Measurement Technology Conference*, 1:969–974, May 1997.